NATIONAL AERONAUTICS AND SPACE ADMINISTRATION

Technical Memorandum 33-525

Fourier Spectroscopy With A One-Million-Point Transformation (Translation)

From the Original Published in the Nouvelle Revue d'Optique Appliquée Vol. 1, pp. 3-22, 1970

Janine Connes and Hervé Delouis
Regional Interdisciplinary Center for Electronic Calculation (CIRCE)

Pierre Connes, Guy Guelachvili, Jean-Pierre Maillard, and Guy Michel
Aimé Cotton Laboratory

National Center for Scientific Research (CNRS)
Orsay Campus
F91-Orsay
France

Translated by
Reinhard Beer
Jet Propulsion Laboratory

JET PROPULSION LABORATORY
CALIFORNIA INSTITUTE OF TECHNOLOGY
PASADENA, CALIFORNIA

March 15, 1972

NATIONAL AERONAUTICS AND SPACE ADMINISTRATION

Technical Memorandum 33-525

Fourier Spectroscopy With A One-Million-Point Transformation (Translation)

From the Original Published in the Nouvelle Revue d'Optique Appliquée Vol. 1, pp. 3-22, 1970

Janine Connes and Hervé Delouis
Regional Interdisciplinary Center for Electronic Calculation (CIRCE)

Pierre Connes, Guy Guelachvili, Jean-Pierre Maillard, and Guy Michel
Aimé Cotton Laboratory

National Center for Scientific Research (CNRS)
Orsay Campus
F91-Orsay
France

Translated by
Reinhard Beer
Jet Propulsion Laboratory

JET PROPULSION LABORATORY
CALIFORNIA INSTITUTE OF TECHNOLOGY
PASADENA, CALIFORNIA

March 15, 1972

Prepared Under Contract No. NAS 7-100
National Aeronautics and Space Administration

TECHNICAL REPORT STANDARD TITLE PAGE

1. Report No. 33-525	2. Government Accession No.	3. Recipient's Catalog No.
4. Title and Subtitle FOURIER SPECTROSCOPY WITH A ONE-MILLION-POINT TRANSFORMATION (TRANSLATION)		5. Report Date March 15, 1972 6. Performing Organization Code
7. Author(s) Janine Connes, Hervé Delouis, Pierre Connes, Guy Guelachvili, Jean-Pierre Maillard, Guy Michel		8. Performing Organization Report No.
9. Performing Organization Name and Address JET PROPULSION LABORATORY California Institute of Technology 4800 Oak Grove Drive Pasadena, California 91103		10. Work Unit No. 11. Contract or Grant No. NAS 7-100 13. Type of Report and Period Covered Technical Memorandum
12. Sponsoring Agency Name and Address NATIONAL AERONAUTICS AND SPACE ADMINISTRATION Washington, D.C. 20546		14. Sponsoring Agency Code

15. Supplementary Notes

16. Abstract

A new type of interferometer for use in Fourier spectroscopy has been devised at the Aimé Cotton Laboratory of the National Center for Scientific Research (CNRS), Orsay, France; with this interferometer and with computational techniques developed by the Regional Interdisciplinary Center for Electronic Calculation (CIRCE) at CNRS, interferograms comprising as many as 10^6 samples can now be transformed. The techniques are described, and examples of spectra of thorium and holmium, derived from 10^6-point interferograms, are presented.

(This Technical Memorandum is a translation of an article, "Spectroscopie de Fourier avec transformation d'un million de points," by J. Connes et al., Nouvelle Revue d'Optique Appliquée, Vol. 1, pp. 3-22, 1970, published by Masson & Cie, Paris, France. The abstract above was prepared by the translator.)

17. Key Words (Selected by Author(s))	18. Distribution Statement
Scientific Instruments Spectrometry	Unclassified -- Unlimited

19. Security Classif. (of this report)	20. Security Classif. (of this page)	21. No. of Pages	22. Price
Unclassified	Unclassified	53	

HOW TO FILL OUT THE TECHNICAL REPORT STANDARD TITLE PAGE

Make items 1, 4, 5, 9, 12, and 13 agree with the corresponding information on the report cover. Use all capital letters for title (item 4). Leave items 2, 6, and 14 blank. Complete the remaining items as follows:

3. Recipient's Catalog No. Reserved for use by report recipients.

7. Author(s). Include corresponding information from the report cover. In addition, list the affiliation of an author if it differs from that of the performing organization.

8. Performing Organization Report No. Insert if performing organization wishes to assign this number.

10. Work Unit No. Use the agency-wide code (for example, 923-50-10-06-72), which uniquely identifies the work unit under which the work was authorized. Non-NASA performing organizations will leave this blank.

11. Insert the number of the contract or grant under which the report was prepared.

15. Supplementary Notes. Enter information not included elsewhere but useful, such as: Prepared in cooperation with... Translation of (or by)... Presented at conference of... To be published in...

16. Abstract. Include a brief (not to exceed 200 words) factual summary of the most significant information contained in the report. If possible, the abstract of a classified report should be unclassified. If the report contains a significant bibliography or literature survey, mention it here.

17. Key Words. Insert terms or short phrases selected by the author that identify the principal subjects covered in the report, and that are sufficiently specific and precise to be used for cataloging.

18. Distribution Statement. Enter one of the authorized statements used to denote releasability to the public or a limitation on dissemination for reasons other than security of defense information. Authorized statements are "Unclassified—Unlimited," "U. S. Government and Contractors only," "U. S. Government Agencies only," and "NASA and NASA Contractors only."

19. Security Classification (of report). NOTE: Reports carrying a security classification will require additional markings giving security and downgrading information as specified by the Security Requirements Checklist and the DoD Industrial Security Manual (DoD 5220.22-M).

20. Security Classification (of this page). NOTE: Because this page may be used in preparing announcements, bibliographies, and data banks, it should be unclassified if possible. If a classification is required, indicate separately the classification of the title and the abstract by following these items with either "(U)" for unclassified, or "(C)" or "(S)" as applicable for classified items.

21. No. of Pages. Insert the number of pages.

22. Price. Insert the price set by the Clearinghouse for Federal Scientific and Technical Information or the Government Printing Office, if known.

PREFACE

The translation presented in this report was performed by the Space Sciences Division of the Jet Propulsion Laboratory.

CONTENTS

CONTENTS (contd)

FIGURES (contd)

ABSTRACT

A new type of interferometer for use in Fourier spectroscopy has been devised at the Aimé Cotton Laboratory of the National Center for Scientific Research (CNRS), Orsay, France; with this interferometer and with computational techniques developed by the Regional Interdisciplinary Center for Electronic Calculation (CIRCE) at CNRS, interferograms comprising as many as 10^6 samples can now be transformed. The techniques are described, and examples of spectra of thorium and holmium, derived from 10^6-point interferograms, are presented.

(This Technical Memorandum is a translation of an article, "Spectroscopie de Fourier avec transformation d'un million de points," by J. Connes et al., Nouvelle Revue d'Optique Appliquée, Vol. 1, pp. 3-22, 1970, published by Masson & Cie, Paris, France. The abstract above was prepared by the translator.)

I. INTRODUCTION

The use of Fourier spectroscopy for problems requiring high resolution is now well established and the advantages have been demonstrated. The development of the technology is pursued at the Aimé Cotton Laboratory and a new type of interferometer has been devised; as a consequence of computational techniques developed by the Regional Interdisciplinary Center for Electronic Calculation (CIRCE) at CNRS, interferograms comprising as many as 10^6 samples can now be transformed.

First, we shall briefly discuss the earlier developments. The first generation interferometer (1964-1966) constructed in collaboration with the Jet Propulsion Laboratory (Refs. 1-3) provided a resolution of up to 0.1 cm^{-1} as a consequence of a carriage movement of 5 cm. It used several novel techniques:

(1) The use of cat's-eye retroreflectors (Ref. 4) in order to eliminate alignment errors caused by the carriage motion.

(2) Step-by-step recording using a servo-controlled carriage, the signal integration being performed when the carriage was stationary. This procedure allowed the path difference to be known to a precision approaching 0.1 nm and used the recording time in an optimum fashion by reducing the number of samples N to the minimum permitted by the sampling theorem (Ref. 1); N therefore becomes equal to the number of spectral elements $M = \Delta\sigma/\delta\sigma$ where $\Delta\sigma$ is the spectral interval being studied and $\delta\sigma$ is the resolution (or width of the instrumental profile). By contrast, workers using continuous scanning must normally use $N>>M$.

(3) Internal modulation of the interferometer (Ref. 3) (that is, modulation of the path-difference itself) at a frequency appropriate to the detector being used. This technique, which gives, approximately, the derivative $dI/d\Delta$ of the interferogram, reduces the effect of intensity variations of the source, particularly those due to atmospheric turbulence. This gives the experimenter a free choice of exposure time.*

The maximum path difference Δ_{max} (= 10 cm) was fixed by the width of the green line of ^{198}Hg used for the servo reference, and the maximum stepping rate (5 steps/second) was determined by the response time of the servo loop. The interferograms were recorded on punched paper tape.

The reductions were performed on an IBM 7040 at the Meudon Observatory; the program used allowed 64,000 points to be transformed (in 105 min). Despite these limitations, the system was well adapted for the study of weak sources such as stars and planets at moderate resolution (0.1--1 cm^{-1}). The planetary spectra were assembled and published as an atlas (Ref. 9).

The MK I interferometer showed that the resolving power and the instrumental function were rigorously identical to the theoretical values. In the meantime, single-mode, frequency-stabilized gas lasers having been developed, it became clear that their use as reference sources would allow Fourier spectroscopy to be extended to very much higher resolving powers.

The MK II interferometer, constructed and tested by J. Pinard (1965-1968) (Refs. 10 and 11) demonstrated the practicability of this extension. The carriage displacement was equal to 80 cm, giving Δ_{max} = 160 cm; the resolution was $\delta\sigma \approx 1/\Delta_{max} = 6 \times 10^{-3}$ cm^{-1}. The new techniques developed were:

(1) The use of the 632.8 nm line from a single-mode He-Ne laser stabilized by the Lamb Dip for a reference source.

*By contrast, the technique called "rapid scanning" (Ref. 5) connects the modulation frequency and the exposure time. Its use on weak sources such as stars requires the summation of a great many successive interferograms in a digital memory. Although well adapted for low-resolution work, it is difficult to use for the kind of problems that interest us.

(2) The use of pressurized oil-bearings for the moving carriage, driven by a two-phase linear motor for the servo; the two approaches are easily extensible to greater movements, and the value of Δ_{max} was chosen only because it seemed adequate for all conceivable studies.

The MK II interferometer was conceived for the study of relatively narrow spectral regions at high resolution. The recording and reduction techniques were essentially the same as for the MK I; since M = N, it follows that the maximum number of spectral elements available was $M_{max} = 64,000$. If $\delta\sigma = 6 \times 10^{-3}$ cm^{-1}, the spectral interval is reduced to 390 cm^{-1}. This instrument, for example, was capable of studying a single vibration-rotation band in the near infrared.

The results obtained established, on the one hand, that the design resolution was attained (it is several times better than that of the best grating spectrometers) and, on the other hand, that the wave-number accuracy was equally improved. In essence, since there is neither scanning of the spectrum nor interpolation between secondary standards, the wave-number scale is determined by purely digital operations based upon a single standard line. In a N_2O band near 4,700 cm^{-1}, an RMS error of 1.5×10^{-4} cm^{-1} was obtained by comparison to the calculated positions (an accuracy of 3×10^{7}).

If even greater resolving powers do not seem to be required, then an increase in the width of the spectral interval to be studied would be feasible and would allow new problems to be attacked at maximum resolution.

It is clear that Fourier spectroscopy will not have shown its full power and the multiplex principle will not be fully exploited until an interferometer can, in a single interferogram, record all the information contained in the spectrum of the source to be studied, within the response range of a single detector.

For example, a recording of an emission spectrum ought to permit the simultaneous measurement of hyperfine structure (and, eventually, the Zeeman structure), isotope shifts, the widths and shapes of the lines, and their absolute positions. For sources of limited lifetime, such as radioactive isotopes (in which we have a great interest), all these data could be obtained in a single run. This is impossible by classical techniques.

In the study of an astronomical source, one tries to obtain the highest resolving power allowed by the available energy in a single observing session; however, the MK I interferometer could only reach $\delta\sigma = 0.1\ cm^{-1}$ at best and this only within one of the three atmospheric windows accessible with a PbS cell (1 to 2.5 μm); hence, three separate runs were needed to cover all this region. As for the MK II interferometer, it was never used astronomically because of the slow recording rate and the narrow spectral interval at high resolution.

Such a goal is much more difficult to attain than a greater increase in resolving power would be since, as we have shown, such an increase would pose no new problems. The problems encountered are of three types:

(1) The difficulty--and duration--of the reduction increases with the number of points to be transformed and is independent of the resolving power.

(2) The rate of controlled movement of the interferometer must be much greater in order to record a given number of data points in a given time. However, the accuracy of the system must be the same; an error of a single step during the scan results in a severe distortion of the spectrum.

(3) The wider the spectral interval and the greater the resolving power, the more the discrimination of the spectral elements (which should, in theory, be perfect in a Fourier transformation) becomes a practical difficulty.

It is useful to introduce a quality factor Q for spectra obtained by Fourier transformation of an interferogram. This is simply the ratio of the total energy

$$\int_0^\infty B(\sigma) \cdot d\sigma$$

contained in a spectrum to that in the minimum detectable line (absorption or emission). With the assumption that the true line width is less than or equal to the instrumental width, the strength of such a line will be essentially

equal to B_{eff}, the RMS value of the random noise in the final spectrum from all causes. The quality factor can therefore be written as $Q = MS_{mean}/B_{eff}$ where S_{mean} is the mean intensity in the spectrum.

The only truly fundamental noise of the system is that of the detector. However, a number of other sources can exist (variations in source brightness, amplifier gain or zero level, instabilities in integrators, digitization noise, etc.) whose relative importance increases as Q becomes larger.

If the factor M is a measure of the superiority of a multiplex technique, then the factor Q is a measure of the difficulties to be overcome in obtaining this gain. The problem which we have attacked here (widening of the spectral interval at high resolution) required just such an increase in Q for the system. The price paid was a greater need for care and a more complex system.

The MK III interferometer, which will be described below, resulted from these various requirements. The step-by-step motion and internal modulation were retained for their proven advantages, while leaving a much wider scope than we had in the earlier systems for a choice of step-length and modulation amplitude and being totally secure against external vibration.

The maximum stepping rate is 50 per second, and 10^6 samples can be recorded, although this last figure is by no means the limit feasible. At the same time, the computational techniques have been developed to transform such an interferogram in 22 min on an IBM 360/75.

II. INTERFEROMETER AND SERVO SYSTEM

A. Optics

The general layout of the MK III interferometer is similar to that of the MK II (Ref. 10, Fig. 2). The maximum carriage movement is 1 meter, whence

$$\Delta_{max} = 2m \text{ and } \delta\sigma = 5 \times 10^{-3} \text{ cm}^{-1}$$

The diameter of the cat's-eyes has been increased from 80 to 160 mm and the useful beam diameter from 20 to 80 mm. The single beamsplitter has been replaced by two separate plates labelled S (splitter) and M (mixer), the thicknesses being identical to within 0.1 μm (Fig. 1). A common support and fine flexure adjustments assure their parallelism. The two semi-transparent coatings were made simultaneously on both plates, assuring their identity and making the system perfectly achromatic. The plates themselves are of Infrasil and the coatings are of silicon, the optical thickness being one-quarter-wave at 1.6 μm; the 4RT product is greater than 0.75 from 0.8 to 3.5 μm. Other plates are planned for other spectral regions.

The reference line used is the xenon superradiant emission line λ_r = 3.50 μm (Section III-A). The beam first passes through a linear polarizer P (2-mm plate of dichroic calcite [calcium carbonate] cut parallel to the optic axis (Ref. 13)). In the two arms of the interferometer are two quarter-wave plates Q_1 and Q_2 (quartz cut parallel to the axis, the thickness being e = 136 μm) orientated in such a way that the beams are right (D) and left (G) circularly polarized; after recombination at M these interfere to give a linear polarization R of constant intensity (independent of Δ). By contrast, the azimuth α of the polarization is a linear function of Δ and rotates through an angle π

for a change in path difference of λ_r; if Δ_0 is a particular value of Δ and α_0 is the corresponding azimuth, one finds that

$$\alpha - \alpha_0 = \frac{\pi(\Delta - \Delta_0)}{\lambda_r}$$

Fixing the interferometer at a particular Δ is equivalent to requiring that α take a given value.

The measurement of α is reduced to the measurement of the phase of a modulated signal. A half-wave plate D, which rotates at constant speed (N turns/second), rotates the transmitted plane of polarization at 2N turns/second. After passing through a fixed linear polarizer A_s (identical to P) the flux is sinusoidally modulated in intensity at a frequency of 4N Hz*. A detector H_s (an uncooled InAs photovoltaic cell) gives a signal F_s at a frequency of 4N Hz which acts as a phase-modulated carrier wave for the path-difference variations in Δ. If the zero of phase occurs when $\Delta = \Delta_0$, then we may write

$$F_s = I \sin 2\pi \left(4Nt + \frac{\Delta - \Delta_0}{\lambda_r}\right)$$

B. Error Signal

From F_s one seeks to produce an error signal, that is, a dc voltage E proportional to the difference $(\Delta - \Delta_0)$; furthermore, it is desirable to reduce the residual ripple of the 4N Hz carrier wave as much as possible.

*This is the same as saying that the half-wave plate increases the frequency of one of the circular polarizations by 2N Hz and reduces the frequency of the other by the same amount; the detector H_s detects the beats between these two frequencies.

The signal F_s is first of all shaped (Figs. 2 and 3) and results in a square wave of the same phase and of unit amplitude C_s. A synchronous demodulator multiplies C_s with a square-wave reference R_s having the same frequency and an adjustable phase whose production is discussed later. The product $P_s = C_s \cdot R_s$ can be considered as a train of positive or negative pulses of unit amplitude, of which the width depends on the relative phase of R_s and C_s. The mean value is zero if C_s and R_s are in quadrature, equals +1 if they are in phase, and equals -1 if they are in opposition. This mean value can be used as an error signal; its variation as a function of Δ (for a given phase of R_s) is shown in Fig. 4: it is linear over a range of $\pm\lambda_r/4$ variation in Δ around the value Δ_0 at which C_s and R_s are in quadrature, the nominal operating point.

However, at this condition there is an unwanted residual ripple superposed which has its greatest amplitude just at the position that $\Delta = \Delta_0$; this ripple is a square wave of frequency 8N and of unit amplitude. In order to suppress it, a second detector H_c is used which receives half of the reference beam by way of a semireflecting mirror L and a second analyzer A_c, which is set at 45 deg with respect to A_s (Fig. 1). A second signal F_c, in quadrature with F_s, is thereby generated; after shaping, it gives C_c, in quadrature with C_s. A second synchronous demodulator generates the product $P_c = C_c \cdot R_c$, where R_c is a second reference signal automatically in quadrature with R_s. The sum $E = P_c + P_s$ is taken and used as the error signal. Figure 2 shows that E is composed of a train of rectangular pulses, identical and equidistant, of constant height, of frequency 16N, of positive or negative polarity depending on the sign of $(\Delta - \Delta_0)$ and of width

$$T = \frac{1}{4} N \cdot | \Delta - \Delta_0 | / \lambda_r$$

When $\Delta = \Delta_0$, $E \equiv 0$ and the carrier is totally suppressed. For $\Delta \neq \Delta_0$, the mean value of the pulses--which is the required information--is once more given by Fig. 4; a residual of the carrier remains but at a frequency 16N; the passband of the servo system is, however, fundamentally much less than 16N. It is equivalent to saying that if, at a

certain instant, a step-function error Δ is imposed upon the rest value Δ_0, the information necessary to make the correction will be unknown until after an error pulse has been received; that is, after a delay which is at most 1/16N. With the value of N = 1000 turns/second finally adopted, this delay equals 0.62×10^{-4} seconds; it is nearly negligible compared to the mechanical response time of the system.

C. Damping Signal

In order to obtain an optimum servo feedback, it is useful to have a damping signal; that is, a second dc voltage E' proportional to $d\Delta/dt$. Noticing that if the path difference changes at constant speed, following a law $(\Delta - \Delta_0) = Vt$, the phase of the signal F_s will vary linearly with time; that is, the frequency of the carrier is changed: it becomes equal to $4N_v = 4N + V/\lambda_r$ (single side-band modulation).

Figures 5 and 6 explain how E' is produced. The signals C_s and C_c come from the infrared detectors at a frequency $4N_v$ (variable with V) and are used to generate two pulse trains I_s and I_c at twice the frequency $8N_v$ (by differentiation and full-wave rectification) displaced one from the other by a half-period. Each pulse-train unlatches a single-shot in which the excited state has a fixed delay $\theta = 1/16N$, which is exactly equal to half the interval between successive pulses $1/16N_v$ when V = 0 and $N_v = N$.

If $N_v < N$, $\theta > 1/16N_v$, and if $N_v > N$, $\theta < 1/16N_v$. The output voltages of the two single-shots are M_c and M_s; the quiescent state corresponds to a voltage of -1 and the excited state to +1. The summation $M_c + M_s$ results in a train of rectangular, equidistant pulses of constant amplitude and of frequency $16N_v$. The pulses are positive if $N_v < N$ and negative if $N_v > N$; their width is

$$T' = \left| 1/16N - 1/16N_v \right|$$

If $|N_v - N| \ll N$, $T' \approx 1/64 \cdot V/N^2 \lambda_r$.

The mean value of the train is therefore proportional to V, and when $V = 0$, $T' \equiv 0$. This mean value constitutes the desired damping signal E'; the carrier ripple, of frequency 16N, is again zero at equilibrium ($V = 0$).

Up till now, we have assumed that the rotational frequency N was perfectly constant. It is easy to compensate for the effect of its variation if the reference signals R_c and R_s are generated from the same device. The frequency is 4N (independent of V) and the pulse train thus produced* is subtracted from the pulse train discussed above (by sending it to the negative input of a differential amplifier). The servo system has two parallel loops. The low-frequency components of the error signal (roughly 0 to 50 Hz) are sent to a linear motor (see Section III-B) which controls the position of the moving carriage (mass = 12 kg). The high frequencies (above 20 Hz) are sent to a pair of piezoelectric elements which carry the small secondary mirrors of the cat's-eyes (mass = 1 g) for which the maximum displacement is ±20 μm; a step function in path difference Δ of ±80 μm can therefore be made without moving the carriage.

D. Reference Signals R_s and R_c

An air-driven turbine with a hollow axis carries both the half-wave plate D and a glass disk V_A upon which are 400 opaque radial sectors. Two small incandescent lamps L_1 and L_2 mounted diametrically opposite each other illuminate two silicon detectors S_1 and S_2 (Fig. 7); a second, fixed, disk V_B is mounted coaxially to V_A. The sum of the two signals from S_1 and S_2 is used to eliminate eccentricity errors.

The signal K thus produced has a frequency of 400N, being 400 kHz if N = 1000 turns/second. The reference signals R_s and R_c are generated by dividing K by a factor of 100. The usefulness of this approach lies in the ability to alter the phase of R_s and R_c by digital methods; the phase can take any one of 100 values incrementable in steps of exactly 1/100 of a

*The mean value of this pulse train varies with N; it can be used to servo-control the rotational frequency of the half-wave plate. To date, a simple control of the compressed air supply giving a frequency stability of about 1% has sufficed.

period. Consequently the operating point $\Delta = \Delta_0$ (corresponding to C_s and C_c being in quadrature with R_s and R_c respectively) can be shifted by hundredths of a reference fringe. The smallest sample step is therefore equal to $\lambda_r/100$ (35 nm).

Figures 7 and 8 explain the technique. The signal K is squared and differentiated. Two 400-kHz pulse trains are thereon switched into the lines A and B by inverters; the pulses A and B are displaced by a half-period and cannot coincide. The pulses A are sent directly to the positive (counting) input of an up-down counter, providing a division by 100; the output pulses actuate two switches which produce the square waves R_s and R_c, automatically in quadrature. The pulses B can be sent by the gates P_+ and P_- to either the positive or the negative inputs of the same counter.

If P_+ and P_- are closed, the frequency of R_s and R_c is exactly 1/100 of that of K (400N/100 = 4N); their phases are constant and the interferometer carriage does not move. If P_+ passes a single B pulse, the phases of R_s and R_c advance by 1/100 of a period and Δ increases by an amount equal to $\lambda_r/100$. If P_- is used, an equal and opposite decrease in Δ is obtained. If P_+ is held open, the frequencies of R_s and R_c become 8N; if P_-, they fall to zero; the interferometer carriage thereupon goes into a constant velocity condition, forward or backward. The corresponding velocity in Δ is $\pm 4N\lambda_r$ (14 mm/s for N = 1 kHz and λ_r = 3.5 μm); this is the maximum (slew) speed that is permitted by the system.

E. Path Difference Scan Program

By means of an appropriate programming method for P_+ and P_-, any path difference scan program $\Delta(t)$ which satisfies the foregoing restrictions (minimum step 35.0 nm, maximum velocity 14 mm/s) can be obtained. In particular, the internal modulation itself can be included into the program and the amplitude controlled by the servo system, which was not the case with the earlier systems.

The program $\Delta(r)$ actually used is represented by Fig. 9. The operating cycle is made up of two parts. During the interval AB the carriage is at rest and the internal modulation is performed by the piezoelectric

elements. Their peak-to-peak amplitude is $q\lambda_r/100$ (where q is integral and $< 10^3$)*; the frequency N' is a submultiple of N (we generally use N' = 250 Hz). The resting time AB (and the integration time for the signal coming from the source) is an integral multiple of the internal modulation period 1/N'. Very short integration times can therefore be used without error (Ref. 2, p. 126).

During the interval BC, Δ increases by $P\lambda_r/100$ (where p is integral and $< 10^4$), the basic step-length, ** and the integrator is reset to zero. The step is produced by a movement of the carriage; however, because of the inertia, it follows the scan program $\Delta(t)$ only after a delay of a few milliseconds, and the piezoelectric elements are used to compensate for this automatically. The maximum scan rate is 200 steps/second.

For problems of a type somewhat different from those envisaged here (intense sources of short lifetime such as plasmas, for example) one might try for a much higher stepping-rate (the number of samples N would not necessarily be greater). The only fundamental limitation would seem to be the response time of the infrared detector being used. However, under these conditions, there would no longer be any reason to keep the step-by-step scan and the internal modulation; the technique of "rapid scanning" (Ref. 5) would seem to be more appropriate. Moreover, there is no discontinuity between the approaches; when the integration time AB becomes equal to a single period 1/N', the recording rate with internal modulation is at its maximum; the (much greater) recording rate becomes, in effect, a rapid scan. Our servo arrangement can work equally well in such a mode but we should need a much

---

*It should be remembered (Refs. 2 and 3) that the amplitude of the internal modulation must equal $\lambda_{mean}/4$, where $\lambda_{mean} = 1/\sigma_{mean}$ and σ_{mean} is the central wave number of the spectral interval under study, and that a square-wave modulation is optimum. However, the advantage over a sinusoidal modulation is small and is not enough to make the effort needed to generate a good square worthwhile. In the near infrared (where we plan to work) the difference is negligible. For instance, if $\lambda_{mean} = 10\ \mu m$, the modulation amplitude is 2.5 μm and the rise time $\theta' = 3.5 \times 10^{-4}$ s is less than a tenth of a modulation period (for N = 1 kHz and N' = 250 Hz).

**The rules for determining the step-length have been given elsewhere (Ref. 12). It may be recalled that it is determined by the limits σ_1 and σ_2 of the spectral region under study; to a first approximation it is of the order of $1/2(\sigma_2 - \sigma_1) = 1/2\Delta\sigma$.

faster incremental recording system than the present one, which is limited to 50 measurements/second (see Section III-E).

F. Advantages of the System

The first advantage is the smallness of the minimum step $\lambda_r/100$ = 35.0 nm, which allows a much more flexible choice of sampling interval than the earlier systems; one may therefore use only the theoretically minimum number of samples N as allowed by the sampling theorem (which is essential when the number is very large). Similarly, the controllable amplitude of the internal modulation allows optimum usage for any spectral region.*

A second, less obvious, advantage is the following: in spite of the smallness of the basic step-length, the functioning of the system is much less susceptible to vibration than the MK I or II because we do not count interference fringes. The counting depends only on the 400-kHz signal, for which the amplitude and frequency are stable to about 1% and the signal-to-noise ratio is very high. Intensity fluctuations in the superradiant tube can in no way introduce a counting error.

The response range** of the servo is rigorously linear over a change in Δ of $\pm \lambda_r/4$ (± 0.88 μm). For the MK I and II interferometers, the error signal was generated starting from the intensity of sinusoidal fringes; with the 632.8-nm line from a He-Ne laser, the useful response range (roughly linear) was about ± 0.1 μm.

These improvements are directly responsible for the improvement in the servo system bandwidth and the gain in speed and security of the entire system; they have allowed us to go from 5 points/second to 200 points/second and from an N of 60,000 to $N = 10^6$.

*The MK II interferometer necessarily used an amplitude that was a multiple of the reference wavelength.

**This range can be increased without limit should the need be felt. Starting from the already available signals C_S, C_C, R_C, and R_S, a second error signal E_1, in quadrature with E, can easily be generated (Fig. 4). The development of E and E_1 starting from a position Δ_0 defines the value of Δ without ambiguity; a reversible period counter on E and E_1 would permit an error signal to be produced that cancels only once (at $\Delta = \Delta_0$).

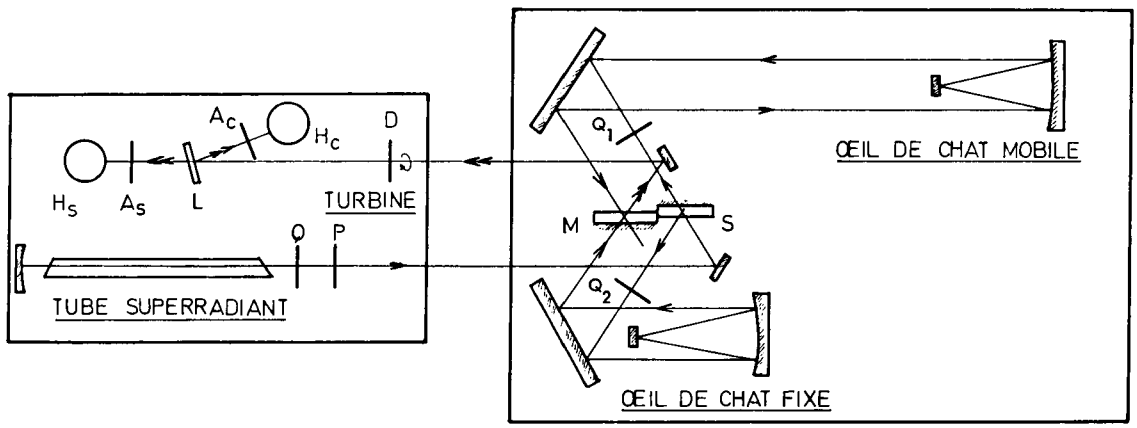

Fig. 1. Simplified schematic of the optical system. Only the reference beam (10 mm diameter) is shown; it travels down the center of the main source beam (80 mm diameter). The interferometer, on the one hand, and the superradiant tube, the turbine and the detectors on the other hand, are mounted on separate baseplates.

NOTE: OEIL DE CHAT = cat's eye

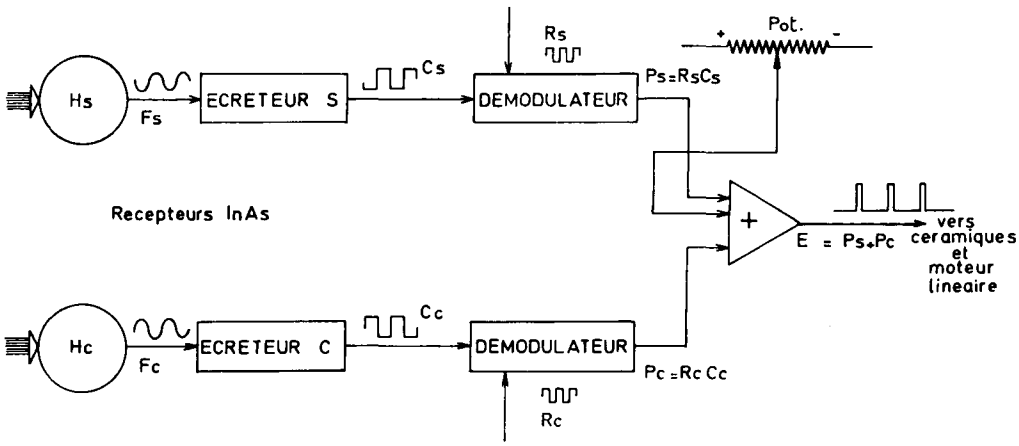

Fig. 2. Method of generation of the error signal $E = P_s + P_c$, starting from the phase-modulated signals F_s and F_c and the reference signals R_s and R_c. The potentiometer P allows a dc voltage to be added to the error signal and a small change in Δ, equal to a fraction of the elementary step-length $\lambda_r/100$, to be produced; it may be directly calibrated in terms of path-difference. It is used to place the first sample in the interferogram exactly at the point $\Delta = 0$.

NOTE: ECRETEUR = shaper

CÉRAMIQUE = piezo-electric element

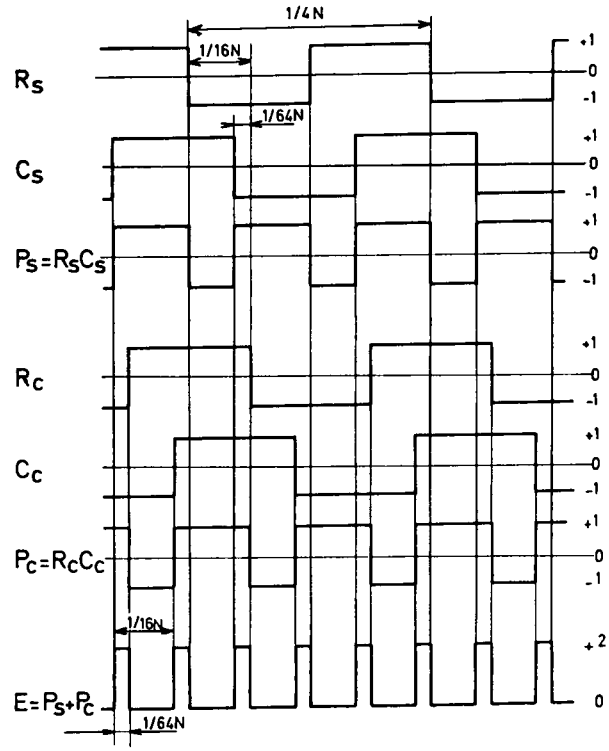

Fig. 3. Waveforms of the signals from which the error signal $E = P_s + P_c$ is generated. The figure illustrates the condition that $\Delta - \Delta_0 = \lambda_r/16$; that is, C_s and C_c are out of phase by 1/16 of the period with respect to the quadrature with R_s and R_c (which would give $E \equiv 0$).

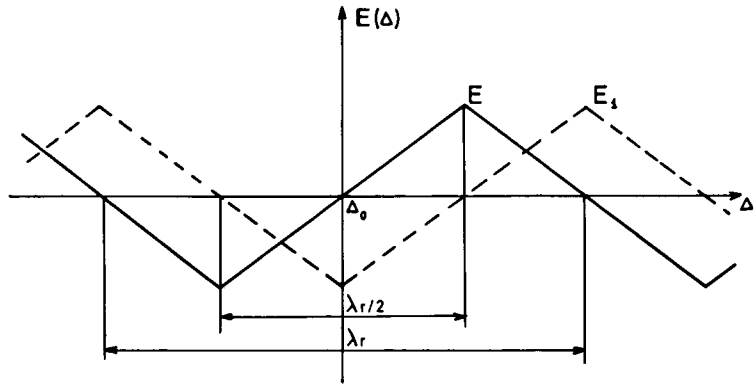

Fig. 4. Variation of the error signal E as a function of Δ around the operating point Δ_0. The phase of the reference signals R_s and R_c is presumed constant. The function is periodic with a period λ_r; it is linear within a range of $\lambda_r/2$. The error signal has the correct sense (and the restoring force is towards Δ_0) over a range of λ_r. A second error signal in quadrature with E is represented by E_1 (see footnote, page 13).

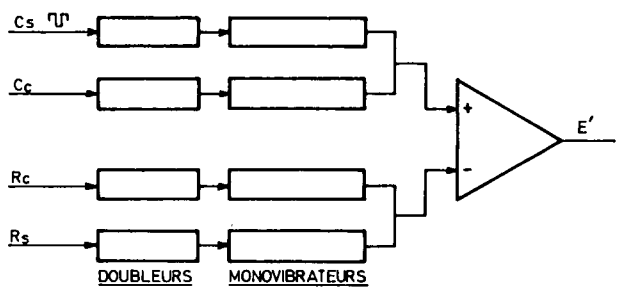

Fig. 5. Generation of the servo feedback signal

NOTE: DOUBLER = frequency doubler

MONOVIBRATEUR = single-shot multivibrator

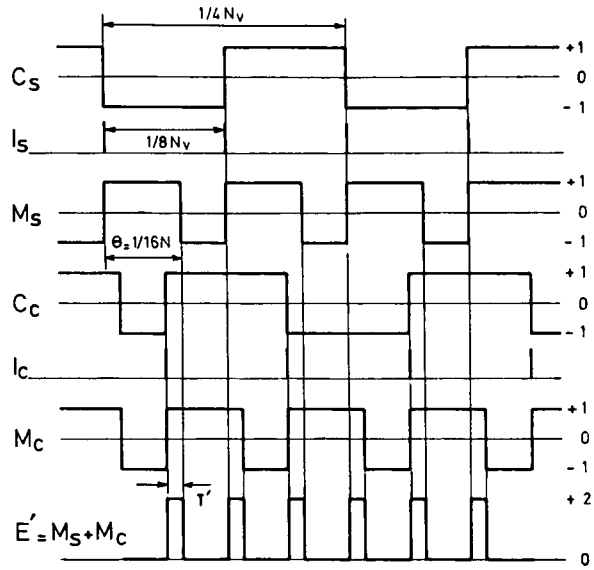

Fig. 6. Waveforms of the signals producing the damping signal E' = $M_C + M_S$. The figure shows the case wherein $N_V < N$.

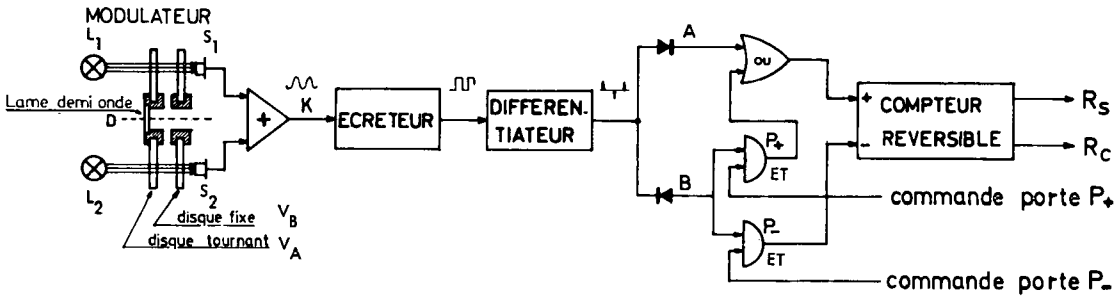

Fig. 7. Generation of the reference signals R_s and R_c at a frequency of 4N.

NOTE: LAME DEMI-ONDE = half-wave plate

DISQUE FIXE = fixed disk

DISQUE TOURNANT = rotating disk

ECRETEUR = shaper

COMMANDE PORTE = gate-open pulse

OU = (logical) OR

ET = (logical) AND

COMPTEUR REVERSIBLE = up-down counter

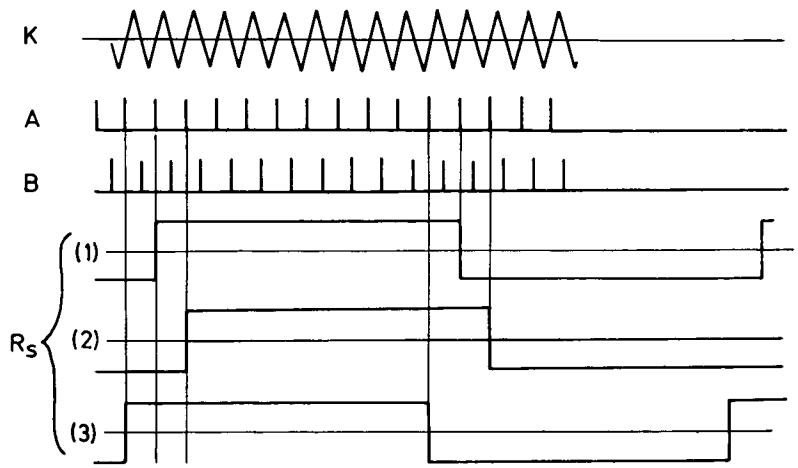

Fig. 8. Reference signals R_s and R_c. Starting from the signal K, at a frequency of 400 N, two pulse-trains A and B are generated. The leading and trailing edges of the square-wave R_s (1) leaving the up-down counter are defined by the pulses A. If the gate P_- allows an extra pulse to pass, the phase of R_s is retarded by 1/100 of the period (R_s (2)); if it is the gate P_+, the phase is advanced by the same amount (R_s (3)). The waveform R_c (not shown) stays in quadrature with R_s. The figure is not to scale, the ratio of 100 between K and R_s not being maintained.

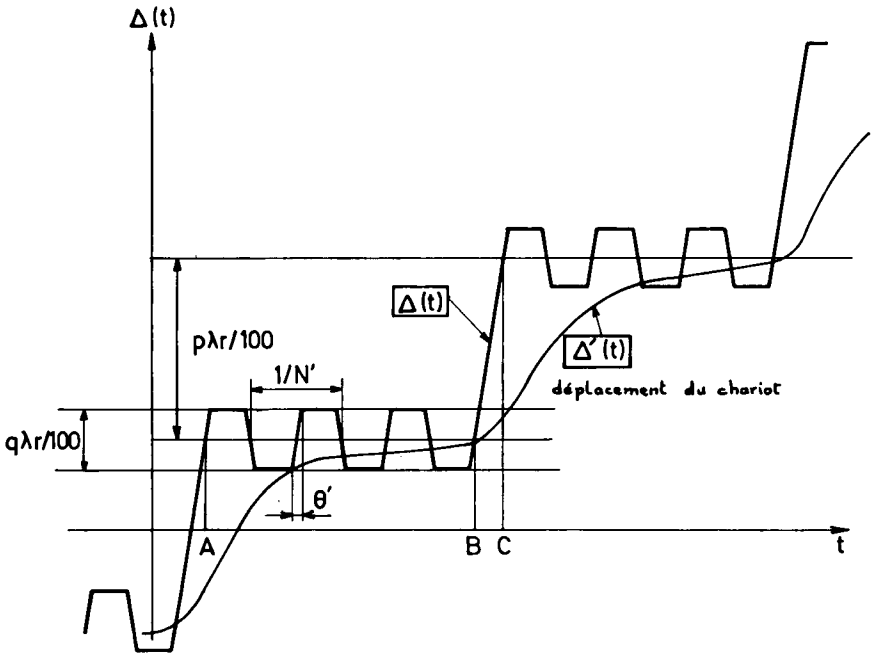

Fig. 9. The function Δ(t). The finite (error) width of the elementary step is neglected in this figure. The symbol Δ'(t) represents the actual carriage motion; the displacements of the small mirrors mounted on the piezo-electric elements are given by Δ - Δ'.

NOTE: DÉPLACEMENT DU CHARIOT = carriage motion

III. BRIEF DESCRIPTION OF THE SYSTEM ELEMENTS

Only the novel items are discussed here; a more detailed description will be given in subsequent publications.

A. Superradiant Xenon Source

This is a tube 1 m long and 3 mm in diameter (just enough to pass the TEM_{00} axial mode at 3.5 μm); the useful length is doubled by virtue of a fully reflecting mirror at one end. Filled either with xenon or a Xe-He mixture and dc excited, this tube emits an intense 3.5-μm line along its axis.

The calculated Doppler width is of the order of 4×10^{-3} cm^{-1} (for 400 K); the effective line width is much less than this because of the superradiance. In fact, neither the width nor the profile have been measured since these parameters do not intervene in the use of the line for a reference; a small reduction in depth of modulation is noticed at $\Delta = 2$ m; this reduction has no effect on the phase modulation system.

The position of the line is not defined by a cavity* and therefore constitutes a natural standard. The principal source of instability appears to be variations in pressure; the pressure is maintained at the saturation vapor pressure of xenon at a well-determined temperature (about 77 K) using a reservoir of xenon submerged in liquid nitrogen boiling under a pressure of about 2 kg/cm^2. To date, only natural xenon has been used and the absolute wavelength λ_r has not been measured. Eventually, ^{136}xenon will be used.

This tube is a convenient reference source for Fourier spectroscopy, much simpler than a single-mode servo-controlled laser. Because of the greater wavelength, the servo control is more certain; furthermore, materials which are not transparent in the visible (germanium or silicon) or which cannot be polished to a sufficient precision (sodium chloride) become usable as beamsplitters.

---

*It is desirable to suppress light reflected back to the superradiant tube by the various optical elements which can result in laser-type action. In our equipment, the quarter-wave plate Q placed in front of the polarizer P (Fig. 1) forms an optical isolator.

B. Linear Motor

The linear servomotor for the MK I interferometer was a simple solenoid in the radial field of an annular magnet; the range (5 cm) was limited by the length of the solenoid. That of the MK II interferometer (Refs. 10 and 11) was a two-phase asynchronous type and the maximum available thrust was only a fraction of a newton force. This type of motor has the inconvenience (important for a system to be operated in a vacuum) of a significant power dissipation (even when the thrust demand is zero) because of the ac polarizing current.

A dc linear motor, with a noncontacting commutator for detection of the field polarity by means of Hall effect detectors, has been employed for the MK III Interferometer (Fig. 10). The maximum thrust available is 40 newtons force for a dissipation of 100 W (this value being the limit of the dc power amplifiers). In fact, the carriage acceleration is found to be limited by mechanical resonances and the maximum thrust is never used. We now think that a linear dc motor of a more classical type (long pole, without commutation) could suffice.

C. Piezoelectric Elements

These are the high-frequency elements of the servo system. Figure 11 shows the layout. They drive the small secondary mirrors of the cat's-eyes. The elements are enclosed in copper tubes; a silicone damping oil (viscosity 0.1 m^2/s) provides simultaneous mechanical damping and thermal dissipation. The whole arrangement can operate in vacuo. The drive for the electrodes comes from high-voltage transformers. The maximum allowable voltage between the internal and external electrodes is 2000 V and produces the 20-μm displacement cited earlier.

D. Rotation of the Half-Wave Plate

A commercial grinder bearing with a hollow axis and driven by compressed air is used for the rotation of the half-wave plate. The noise level and the vibration are tolerable and cause no particular problem. However, the lubrication (and lifetime) of the ball-races is unsatisfactory: the use of a rotary air-bearing should resolve this difficulty.

E. Measurement and Recording Arrangement

Figure 12 shows a simplified schematic of the system arrangement. The signal to be measured is demodulated by a 250-Hz square wave, of adjustable phase, synchronous with the internal modulator. Integration is performed by a voltage-to-frequency converter followed by a 5 decimal digit up-down counter; the samples are stored and a new integration begun during the writing-time on the magnetic tape of the previous sample. Each measurement involves the recording of 6 binary coded decimal (BCD) characters, one of which is a flag character indicating the gain of a manually operated 4-position attenuator (gain of 1, 10, 100, 1000); its purpose is to augment the dynamic range of the system (Ref. 2).

The total intensity of the source under study is determined by a detector R', and a voltage proportional to it is sent to a conventional potentiometric recorder P, which gives a permanent indication of it. A second potentiometer, coupled to the first, is introduced into the feedback loop of a variable-gain amplifier; source intensity fluctuations are thereby compensated (on the assumption that they are achromatic, of course).

The recorder is of the incremental type* (400 steps/second). When 6 characters are recorded, taking dead-time into account, the maximum rate is 50 points/second.

F. Adjustments

The system of phase modulation is, by its very nature, insensitive to intensity variations in the reference signal; it requires neither a delicate balance between two different detectors, nor manipulation of precise

*Step-by-step recording allows stops of any length to be made during a recording. Thus magnetic tapes directly readable by a computer can be made, which must necessarily be composed of data records separated by gaps. If the interferometer ran continuously, a buffer store would be necessary.

waveforms by very linear circuits;* the analog part is reduced to an absolute minimum (preamplifiers) and all subsequent operations are digital. However, it must be expected that any system of path difference measurement not operating by simple counting of whole fringes (and thereby allowing an estimate of the fractional error to be made) must introduce a periodic error of period λ_r; ours is no exception.

Imperfections of the optical system have two different consequences:

(1) The calcite dichroic linear polarizers are of very high quality (Ref. 13), but by contrast the thickness of the quarter-wave plates is accurate only to about 1%. To try to get better precision would be pointless, because the number of oblique reflections in both the interior and the exterior of the interferometer, not to mention the oblique transmission through the plates S and M, causes the interfering vibrations to be deformed so that the polarization becomes elliptical instead of circular.

It is fortunately possible to compensate for all these errors without measuring them individually, by making the incidence on the quarter-wave plates Q_1 and Q_2 slightly oblique. This compensation is very delicate; it requires, in effect, a simultaneous 3-parameter adjustment (azimuth of the quarter-wave plate in its plane, the angle of incidence and the plane of incidence). It is performed by occulting one of the beams in the interferometer and orientating the quarter-wave plate in the other beam in such a way as to annul the modulated signal received by either of the detectors H_s or H_c; the incident vibration on the rotating half-wave plate is then necessarily circular.

*These qualities, which are essential for a precise measure of Δ, are a property of the mechanical system which produces the modulation (rotating halfwave plate D mounted rigidly to the disk V_A). Of course, it is possible to perform the equivalent operation with electro-optic crystals driven by suitable sinusoidal voltages. But in order to obtain a rigorous relationship between the phases of the reference signals of frequency 4N and 400N, an extreme precision in the waveforms and amplitudes of the applied signals, not to mention the driving conditions and the crystal temperature control, would be necessary. An alternative measurement system, somewhat like ours (Ref. 14), in which the carrier is obtained by beats between the Zeeman components of a laser line, has the advantage of not requiring a rotating element. But it no longer allows the fine, accurate, and rapid interpolation between whole fringes which is the essential property of our arrangement.

This empirical adjustment is convenient only if it is possible to follow the phase and the amplitude of the modulated signal; therefore, the signal (before squaring) is sent to two synchronous demodulators fed by the reference signals R_s and R_c. Their dc outputs are fed to the X and Y inputs of an oscilloscope and one attempts to center the spot. The accuracy of the adjustment is limited by the signal-to-noise ratio of the reference signal; an ellipticity of less than 1.5×10^{-4} has been obtained, which corresponds to a periodic error ϵ of the order of 0.5 nm in the path difference. Such an error must introduce ghosts into a spectrum calculated by Fourier transformation* for which the spacing from the main line equals $\sigma_r = 1/\lambda_r$ and the intensity is calculated as $2\pi\epsilon/\lambda$. The measured ghost intensity for a visible line (λ = 632.8 nm) was 5×10^{-3}; since it is proportional to $1/\lambda$ it is much reduced in the infrared. This intensity can appear relatively large; but (because of the use of a phase-sensitive Fourier Transform) the resultant shape of the ghosts is asymetric and they cannot be confused with normal lines.

(2) The adjustment of the incidence angle on the rotating half-wave plate D is significantly more delicate. But the error in Δ introduced by the error in the optical thickness of D is time-periodic (of period 1/N). Since the internal modulation period 1/N' and the integration time is an integral multiple of 1/N, the average residual effect on each interferogram sample is nil; in other words, only the form of the internal modulation program is (very slightly) changed and is unimportant.

*Since the periodic error is stable, one might imagine measuring it and compensating in order to reduce the ghosts even more. One can, for instance, add a dc voltage, which is a function of the fractional error in the reference fringes, to the error signal. One can also introduce a correction into the computer reduction program; these two approaches have not yet been tried.

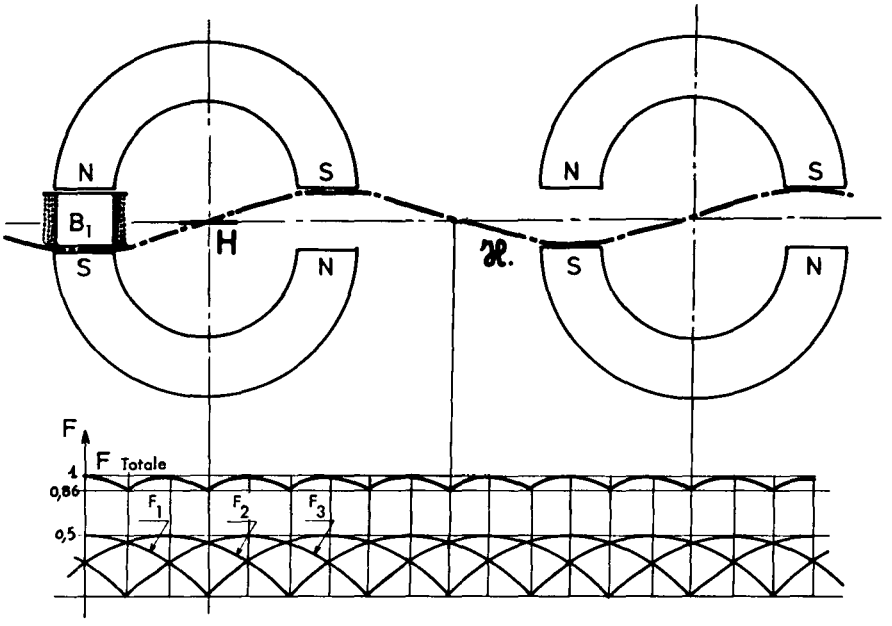

Fig. 10. Direct current linear motor. The interferometer carriage carries a coil B and a Hall effect probe H. Two series of stationary permanent magnets are mounted on each side of the coil in the direction of motion. The magnetic field is periodic; the size of the pole-pieces and of the coil are such that the force generated with a constant current is nearly sinusoidal. The probe senses the zeros of the field and causes the coil current to be reversed; the curve showing the force as a function of displacement is therefore the rectified sine-wave F_1. Three identical combinations (coil and probe) are used, simultaneously, displaced by 1/3 of a period, giving the forces F_1, F_2, and F_3. The resultant force F_T is thereby only slightly modulated.

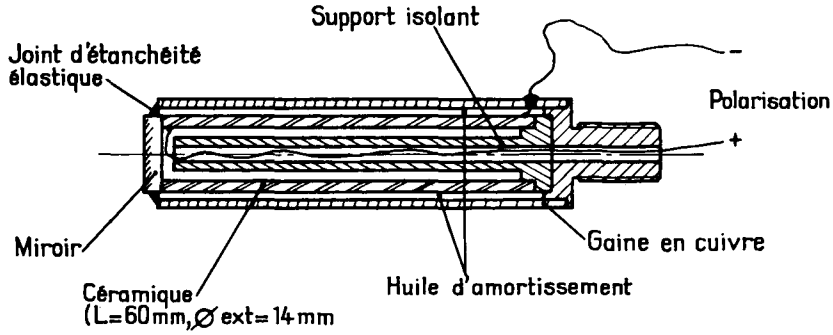

Fig. 11. Mounting of the piezo-electric elements

NOTE: JOINT D'ÉTANCHÉITÉ ÉLASTIQUE = watertight, elastic, joint

SUPPORT ISOLANT = insulated support

POLARIZATION = power leads

GAINE EN CUIVRE = copper sleeve

HUILE D'AMORTISSEMENT = damping oil

CÉRAMIQUE = piezo-electric tube

MIROIR = mirror

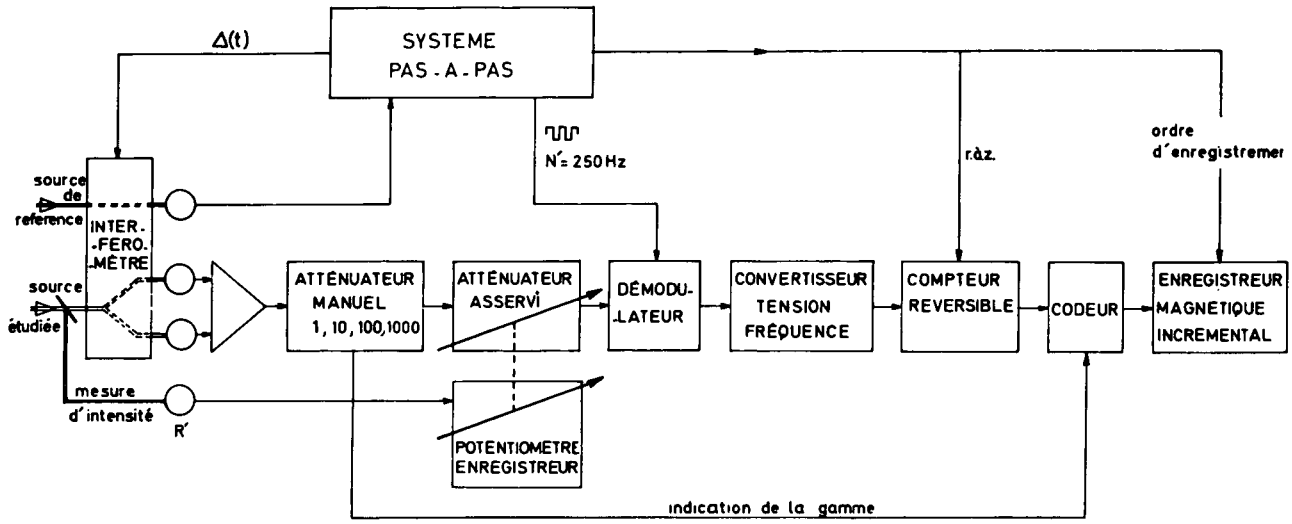

Fig. 12. Schematic of the measuring and recording system (analog and digital parts)

NOTE:

SOURCE DE REFERENCE	=	control laser
SOURCE ETUDIÉE	=	source being measured
MESURE D'INTENSITÉ	=	total input power monitor
SYSTEME PAS-A-PAS	=	step-and-lock logic
ATTENUATEUR MANUEL	=	manual attenuator
ATTENUATEUR ASSERVI	=	servo-controlled attenuator
POTENTIOMETRE ENREGISTREUR	=	potentiometric strip-chart recorder
CONVERTISSEUR TENSION-FREQUENCE	=	voltage-frequency converter
R.À.Z.	=	reset to zero
INDICATION DE LA GAMME	=	gain indication
COMPTEUR	=	counter
CODEUR	=	encoder (coupler)
ORDRE D'ENREGISTREMENT	=	write command

IV. METHODS OF REDUCTION

The problems of the reduction process can be classified into two categories:

(1) The calculation of a clean Fourier Transform (FT).

(2) Various operations performed on the recorded interferogram before calculation of the FT; interpolation of the output spectrum between the calculated primary points after the FT; plotting the spectra and their exploitation.

Following the programming of the mathematical principles involved in the treatment of the interferogram and of the spectrum, the principal difficulty lies in the number of data points to be manipulated, which is always greater than the size of the core of a computer. We have transformed 60,000 points with an IBM 7040 having a 32K word* core. We now have a 360/75 having 256K words but we need to transform 10^6 points.

Now, the fast FT method of Cooley and Tukey is easily applied when all the computation can be done in core. However, when the number of points exceeds a limit N_L, depending on the computer being used, auxiliary stores (tapes or disks) must be used, for which the access time is much greater than that for the core. It has been necessary, therefore, to generate two programs for transforming a number of points which, in one case, is less than N_L and in the other, is greater.

A. Calculation of the Fourier Transform

We must calculate the sine FT of an odd function sampled by N points between $\Delta = 0$ and Δ_{max}. Let us put

$$h = \frac{P\lambda_r}{100} = \frac{1}{2\Delta\sigma}$$

*$1K = 2^{10} = 1024$.

where h is the distance between sample points (Fig. 13). Starting from the N samples of the interferogram I (Δ), one calculates N samples of the spectrum S (σ) separated by $\delta\sigma$ by the series

$$S(\sigma_1 + p\delta\sigma) = \sum_{k=1}^{k=N} I_{k-1} \cos [2\pi(\sigma_1 + p\delta\sigma)(k-1)h]$$

1. Classical method. The classical algorithm using this formula leads, for the calculation of the N points in the spectrum, to the product of a square matrix of rank N by a column matrix of N terms, wherein the calculation time is proportional to N^2 and the coefficient of proportionality is dependent on the computer used and the method of generating the cosines. The best times realized follow the formulae

$$T = 0.8 \times 10^{-3} N^2 \text{ for an IBM 704}$$

and

$$T = 0.3 \times 10^{-3} N^2 \text{ for a 7040}$$

with T being expressed in seconds (Fig. 14 and Table 1).

In practice, the largest scale on which this algorithm was used was for the calculation of spectra of Jupiter (1965) with N = 12,000 in 12 h.

2. Cooley-Tukey method. In its original form, this method permits the calculation of the Fourier Transform of any kind of complex function. Thus, in our notation, $N_D = 2N$ complex samples are transformed in order to obtain N_D complex values of the spectrum spread out in the interval $2\Delta\sigma = 1/h$.

The general idea of the method was expressed at the beginning of the fundamental paper by Cooley and Tukey (Ref. 24): "the square matrix $N_D \times N_D$ can be considered as the product of m partially-filled matrices, m being equal to $\log_2 N_D$."

a. Complex functions. In this case, the necessary core size is $2N_D$ words, which implies reserving 4N words for the 2N real samples taken

between $-\Delta_{max}$ and $+\Delta_{max}$* and 2N imaginary, null values. Let H be the size of the memory of the computer under consideration; H is always a power of 2. Since a portion is necessarily taken up by the system monitor and the program, one can, at most, use H/2 words for storing the data; therefore with a 7040 with a 32K core one can, at most, handle an interferogram of

$$N_L = \frac{H}{2 \times 4} = 4K = 4096 \text{ words}$$

With a 360/75 with a 256K core, N_L becomes 32K.

On the other hand, the results of the FT are not in order and the elementary sorting by inversion of the bits adds a term in N_D^2 to the calculation time which is quite negligible for small N_D but becomes dominant for large N_D. An improvement of the sorting method has required the use of an extra N_D words in the core but has suppressed the term in N_D^2. Two equivalent programs, an FFT for 4K words and an FFT for 32K words, have been written for a 7040 and a 360/75 and have resulted in the following calculation times, in seconds, respectively:

$$T = 9.428 \times 10^{-3} N_D \log_2 N_D + 0.166 \times 10^{-2} N_D$$

and

$$T = 0.152 \times 10^{-4} N_D \log_2 N_D + 0.145 \times 10^{-3} N_D$$

It should be noted that the terms in $N_D \log_2 N_D$ and in N_D are comparable and that the change from a 7040 to a 360/75 gave a speed gain of 23 (see Fig. 14).

b. Real functions. It is possible to convert the calculation of the FT of a real function I', sampled at N_D points, to the calculation of the FT of a complex function I'' sampled at $N_D/2$ points (Ref. 25). The real part of I''

*It may be shown that this is equivalent to writing (in the core array reserved to the real values) N samples taken between 0 and Δ_{max} followed by N zeros.

comprises the samples of even position and the imaginary part those of odd position. Afterwards, it is necessary to re-order either the first $N_D/2$ real samples or the last $N_D/2$ of the spectrum of I', depending on the position of the spectrum to be studied in the free spectral interval 1/h, starting from the $N_D/2$ complex values of the spectrum of I''. By applying this technique, we have written a 64K FFT program for the 360/75 which has two advantages over the earlier methods: it uses only 2N words of memory for storing the data, thereby allowing us to handle N_L = 64K within the central processing unit, and the execution time for a given N is divided by 1.5. The time formula (in seconds) is

$$T = 0.158 \times 10^{-4} N \log_2 N + 0.206 \times 10^{-3} N_D$$

c. Extension of the Cooley-Tukey method for the case of $N > N_L$. In order to handle the case of N > 4K with the 7040 or the case of N > 64K with the 360/75, auxiliary storage must be used. On the other hand, at each stage of the Cooley-Tukey method, the numbers to be handled in succession are not stored sequentially in the memory, so that it is not possible to use the all-encompassing prior programs directly. A different program was written for the 7040. It used four magnetic tapes and the final sorting was not done by bit-inversion but by a formula from which the position of each output sample could be calculated. The running time is given by the expression

$$T = 0.228 \times 10^{-2} N_D \log_2 N_D + 0.747 \times 10^{-2} N_D$$

If N = 64K, T = 105 min. It would be possible to make a significant reduction in the coefficient of the first term but this was not done because a much more powerful computer became available.

For the 360/75, we have written a Fourier Transform program for 1000K points using the so-called "decimation in time" technique (Ref. 26), which allows an FT of a real function, sampled at $N_D = 2^N$ points, to be calculated on a computer having only $N_D/12$ words of fast-access memory.

In the first stage, the N_D samples are sorted and separated into 16 blocks of length $N_D/16$. These blocks are stored on direct-access

locations on a magnetic disk. In the second stage, the Fourier Transform of each of these blocks is calculated, in succession, with a 64K FFT program. The third and final part comprises a series of four stages of intercombining the numbers thus produced. This allows the reconstruction of the FT of the whole. The spectrum samples ($N_D/2$ for the real part and $N_D/2$ for the imaginary part) are thereby ordered sequentially on two locations of the disk.

The total execution time is the sum of the execution times (T_1, T_2, and T_3) of the three parts:

$$T_1 = 0.562 \times 10^{-4} N_D$$

$$T_2 = 0.151 \times 10^{-4} N \log_2 N + 0.206 \times 10^{-3} N_D$$

$$T_3 = 0.336 \times 10^{-3} N_D$$

whence

$$T = 0.151 \times 10^{-4} N \log_2 N + 0.119 \times 10^{-3} N$$

giving for

$$N = 1024\,K, \quad T = 22 \text{ min, } 08 \text{ s}$$

More than half the time is used in the manipulation of the numbers, which explains why, starting from N = 32K, the time increases proportionally to N.

The size and number of locations has been specifically tailored to the case of N = 1024K and is particularly mismatched for $N \leq 64K$, but then one may use the normal 64K FFT. A factor of 3.4 is lost in execution time in going from a 64K in-core calculation to that using disks, but the core usage is 5N/2 in the first case and is only 5N/32 in the second.

Examination of Fig. 14 shows the progress that has been made, thanks to the evolution both of computers and of computing techniques. Fourier Transform spectroscopy is no longer classified in the group of techniques that are gross consumers of machine time.

These figures are not optimum. The first improvement that can be made is to adapt the FFT algorithm to the particular case of a real function which is partly even and partly odd. It is reasonable to expect that this would result in less memory being used and the computation time being reduced.

B. Auxiliary Calculations

The calculation of the Fourier Transform itself is only one stage in the complete treatment which the interferogram must undergo between recording it on magnetic tape and plotting the final spectrum. As was discussed earlier, the interferogram is sampled at the minimum possible number of points N. Consequently, the spectrum obtained by the Fourier Transform is also sampled at N points, N always being a minimum. This signifies that there is only 1 point per spectral element; a linear interpolation gives only a rough approximation to the true spectrum and a precise interpolation scheme (by convolution) is indispensible (Ref. 1).

The computation is performed as follows: the 1024K primary spectral points $S(\sigma)$ resulting from the FT are stored on disk. The search for the maximum value of S takes 25 s; the normalization of all the spectrum and the writing of it onto magnetic tape in 1K records takes 86 s; the calculation of the requisite interpolation function $f(\sigma)$ and various necessary initializations uses another 25 s. At this point, the interpolation proper begins; one may calculate either the entire spectrum or an arbitrary portion; the complete calculation, employing 5 secondary points per primary point, giving $5 \times 1024K \approx 5 \times 10^6$ points, takes 22 min, 10 s.* Finally, the writing of the magnetic tape for the Calcomp 563 plotter is performed in 10 min.* The total time for these operations is thus 1 h, 03 min.

*New software from the plotter manufacturer should allow us to reduce this time.

C. Test Program

It is very useful to have information on the quality of the spectrum as soon as possible after the recording of the interferogram. For this it suffices to calculate, at maximum resolution, three narrow regions (8K points wide, for instance) in three different spectral intervals; one in a region of maximum signal, within which are narrow lines, and the two others at the wings of the spectrum, where the signal is zero; one has, therefore, a simple means of determining the effective noise level and the signal/noise ratio in the spectrum. The calculation of the FT is done from a secondary interferogram sampled at 8K equidistant points spaced at 1024K/8 intervals generated by a suitable convolution with the 10^6 primary samples (Ref. 8). Table 2 gives the corresponding calculation times.

Thus, using a test taking 3×96 s = 4 min 48 s, one has enough information about the spectrum to decide whether to perform the complete calculation.*

*One can, equally well, calculate a complete spectrum of 1024K in 16 slices of 64K if one has access to an "Array Processor," a specialized device for performing convolutions which works in parallel to the Central Processing Unit (CPU). The time for calculating the secondary interferogram then becomes 50 s, whence one may reduce an entire slice of 64K points in 50 + 33.84 ≈ 89 s and the entire spectrum in 24 min. The Array Processor also reduces the time to interpolate the secondary spectral points from the 10^6 primary points from 22 min to 40 s. These trials were performed on an Array Processor connected to the 360/65 at the French National Institute of Astronomy and Geophysics.

Table 1. Calculation times for various machines and programs. The number of samples in the interferogram from a path difference of 0 to Δ_{max} is N.

NOTE: ORDINATEUR = computer

PLACE EN MEM. CENTR. = core used

Ordinateur	704	7040 32 *K*	7040 32 *K*	7040 32 *K*	360/75 256 *K*	360/75 256 *K*	360/75 256 *K*
Programmes	classique	classique	FFT 4 *K* $N < 4$ *K*	avec bandes magnétiques	FFT 32 $N < 32$ *K*	FFT 64 *K* $N < 64$ *K*	TF 1 000 *K* avec disques
Fonction	réelle	réelle	complexe	complexe	complexe	réelle	réelle
Place en mém. centr.	4 *N*	4 *N*	5 *N*	5 *N*	5 *N*	5 *N*/2	5 *N*/32
$N = 0{,}5$ *K*	3 mn 30 s	78 s	7,22 s		0,30 s	0,22 s	
$N = 1$ *K*	14 mn	5 mn 14 s	15,33 s		0,66 s	0,44 s	3,7
$N = 2$ *K*	55 mn 55 s	20 mn 58 s	32,45 s		1,34 s	0,90 s	5.18
$N = 4$ *K*	3 h 43 mn	1 h 23 mn	68,41 s	5 mn 15 s	2,88 s	1,85 s	8,14
$N = 8$ *K*	14 h 56 mn	5 h 35 mn		9 mn 30 s	5,85 s	3,82 s	13,32
$N = 16$ *K*				21 mn	12,22 s	7,86 s	22,94
$N = 32$ *K*				50 mn	25,45 s	16,00 s	42,92
$N = 64$ *K*				1 h 45 mn		33,44 s	1 mn 24 s
$N = 128$ *K*				3 h 32 mn			2 mn 46 s
$N = 256$ *K*							5 mn 27 s
$N = 512$ *K*							11 mn
$N = 1\,024$ *K*							22 mn 08 s

Table 2. Calculation times for slices of 8 K, 32 K, and 64 K spectrum-primary points starting from 10^6 interferogram samples.

NOTE: TF = FT = Fourier Transform

	8 *K*	32 *K*	64 *K*
Calcul de l'interférogramme secondaire	82 s	166 s	265 s
Calcul de la TF.....	3,82 s	16 s	33,44 s
Interpolation dans le Spectre...	10 s	40 s	80 s
Temps total	95,82 s	222 s	378,44 s

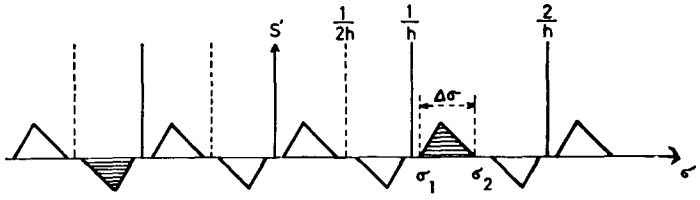

Fig. 13. The actual spectrum occuping the interval $\Delta\sigma$ between σ_1 and σ_2. In the calculation from the samples I(Δ), not only is the spectrum found, but also its images (aliases).

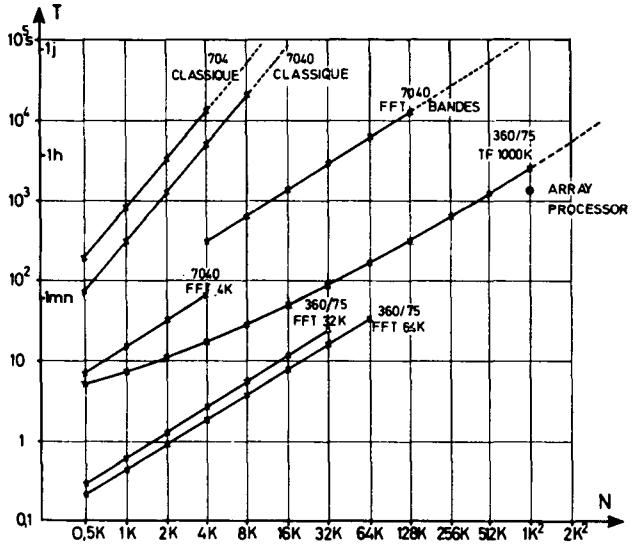

Fig. 14. Plot of the calculation time for various machines and programs. The crosses are measured values. Dotted lines indicate extrapolations.

Author's erratum: In order to agree with the text and Table 1 (which contains the most recent results), the curve for the 1000 K transform on a 360/75 should be lowered by a factor of 2.

V. PRELIMINARY RESULTS

A. Description

Three almost identical interferometers are under construction: one for astronomical spectroscopy, one for laboratory absorption spectroscopy, and one for emission spectra in the laboratory. Only this latter has produced results, to date. The properties of very high resolution and precise frequency measures for this class of instrumentation having been demonstrated (Ref. 11), we now wish to explore the possibility of detecting very weak lines over a wide spectral range and in the presence of a considerable total energy.

The sources used for the study of rare-earth spectra are magnetron-excited electrodeless discharge tubes; they have been difficult sources for Fourier spectroscopy until now. They are frequently very unstable and are particularly prone to go into a low-frequency oscillation at frequencies similar to the sampling-rate and the internal modulation. Under such conditions, the fundamental noise limit of the detectors themselves has yet to be reached. Appreciable improvement can be made by a constant-intensity servo-control of the source itself.

Figures 15, 16, 17, and 18 show various portions of a spectrum of thorium generated from the same interferogram. The recording time used was 10 h (the minimum possible would have been 6 h) the step-length between samples was 0.455 μm (corresponding to p = 13). Consequently, the free spectral range $\Delta\sigma$ goes from 0.91 μm to infinity (0 to 11,000 cm^{-1}). The occupied spectral range is limited by the transparency of the silica envelope of the source (and the response of the PbS detectors) to 3.3 μm (3000 cm^{-1}).

A filter eliminates wavelengths less than 0.8 μm. The lines contained in the interval 0.8 to 0.91 μm (12,500 to 11,000 cm^{-1}) appear in the output in the region 11,000 to 9,500 cm^{-1}; but as a consequence of the properties of a sine transform they appear negative and are very easy to distinguish from the others on high-resolution plots. An absorption spectrum, by contrast, could not be recovered in this manner.

The peak-to-peak amplitude of the internal modulation is equal to 0.70 μm (q = 20). The efficiency is unity at λ = 1.70 μm (6,150 cm^{-1}) and is greater than 0.5 from 2,400 cm^{-1} (4.2 μm) to 12,000 cm^{-1} (0.83 μm).

To summarize, the spectral region 0.8 to 3.3 μm is covered in a single recording at an acceptable efficiency and with no ambiguity in the interpretation. Absolutely no prior knowledge of the spectrum is needed. The PbS detector is not the best possible for use below 1.1 μm, but a useful output in a region already studied (in part by spectrographs) is thereby obtained.

Figure 15 shows the entire spectral region computed from the first 10^4 points of the interferogram; thus the resolution is a factor of 100 worse than the final value. It allows an appreciation of the density of the spectrum. It should also be noticed that the continuous background has atmospheric water vapor absorption bands* near 3700 cm^{-1} and 5400 cm^{-1} superposed on it. The background reaches a maximum at 3660 cm^{-1}. A fraction of the emission lines are due to iodine liberated by decomposition of the thorium iodide used in the source tube.

Figure 16 shows a slice of 400 cm^{-1} computed from the first 10^5 points of the interferogram, and finally 40 cm^{-1} computed using all the interferogram (10^6 points). The maximum path difference attained was 45 cm; with the particular apodizing function used, the resolution was $\delta\sigma = 20 \times 10^{-3}$ cm^{-1}. The line-widths measured in the spectra varied from 40×10^{-3} cm^{-1} near 10,000 cm^{-1} to 25×10^{-3} cm^{-1} near 4,000 cm^{-1}.

Figure 17 shows the profile of an isolated line near 4200 cm^{-1}, and Fig. 18, a very weak line near 3439 cm^{-1} (2.93 μm) superposed on a background which shows H_2O absorption (and noise).

The reproducibility of weak lines is demonstrated in Fig. 16 by comparison of two separate recordings. The differences in intensity are due to differences in the operating mode of the source, which is not precisely reproducible. All the plots are automatically normalized with respect to the strongest line in the spectrum (8,904 cm^{-1}). With respect to this line, the measured effective noise level (in a region of zero signal) $B_{eff} = 0.8 \times 10^{-4}$; from the measure of the total energy in the spectrum, it is deduced that $Q = 10^7$.

*It is planned, eventually, to operate the system in a vacuum. [Translator's note: this was completed by July, 1971.]

Figure 19 shows results obtained with holmium; the recording conditions (N, p, q, $\Delta\sigma$, $\delta\sigma$) were identical. A piece of the spectrum at low resolution (10^4 points) is again presented; the high-resolution spectrum shows the characteristic eight-component structure for holmium (spin 7/2). The measured value of the Q-factor is 2.5×10^7; the highest value obtained previously was 3×10^6 (Ref. 2).

B. Comparison With Results Obtained by Classical Techniques

The study of rich line spectra is relatively easy in the visible region where a large grating spectrograph (Paschen-Runge or crossed-dispersion echelle grating) allows the entire spectrum to be recorded in a single exposure. Many lines of thorium, on the other hand, have been measured photographically with Fabry-Perot etalons and make very useful secondary wavelength standards (precisions of the order of 10^{-3} cm^{-1}) (Ref. 16).

In the infrared, the only technique extensively used to date has been by scanning with a grating spectrometer. Steers (Ref. 17) recorded the thorium spectrum from 1 to 2.5 μm with an echelle grating; about 1000 lines were determined; the measured wave number errors varied from $\pm 2 \times 10^{-2}$ cm^{-1} to $\pm 1 \times 10^{-1}$ cm^{-1}

A scanning Fabry-Perot interferometer gives much better precision; it has been used for noble gas spectra (Ref. 18). Since a separate recording is needed for each line, the method is slow and has not yet been employed for rare earths.

At the Aimé Cotton Laboratory, rare earth spectra are systematically explored with two grating interference spectrometers of the SISAM variety (Ref. 15), with which the speed gain over classical grating spectrometers is already significant. The technique and some results have been discussed by J. Verges (Refs. 19, 20, 21, and 22); the accent has been more on high resolution for the analysis of hyperfine structure, isotope shifts, and Zeeman effect rather than precise absolute positions. The method goes in two successive stages:

(1) A preliminary scan of the entire spectrum is performed at 0.2 cm^{-1} resolution using a first SISAM; the region covered is

4,000 to 12,000 cm^{-1}. The effective recording time is of the order of 150 h and the operation takes about 3 weeks.*

(2) After a first look at the spectrum, in the course of which the interesting lines are noted, an analysis at much higher resolution (0.03 cm^{-1}) is performed in very narrow spectral regions. The effective recording time for one structure is of the order of 10 to 30 min; as a consequence of necessary adjustments and calibrations, the number of structures analyzed does not exceed 10 to 15 per day. The study is necessarily limited to the strongest lines only (50 in the case of holmium, for example). Figure 20 compares the weakest line satisfactorily recorded with the SISAM to the result obtained by Fourier Transform spectroscopy. The intensity of this structure is about 25 times greater than the weakest structure discernible in Fig. 19 (at 8152 cm^{-1}).

*A similar study at longer wavelengths is performed by C. Morillon using a Girard grille spectrometer (Ref. 23).

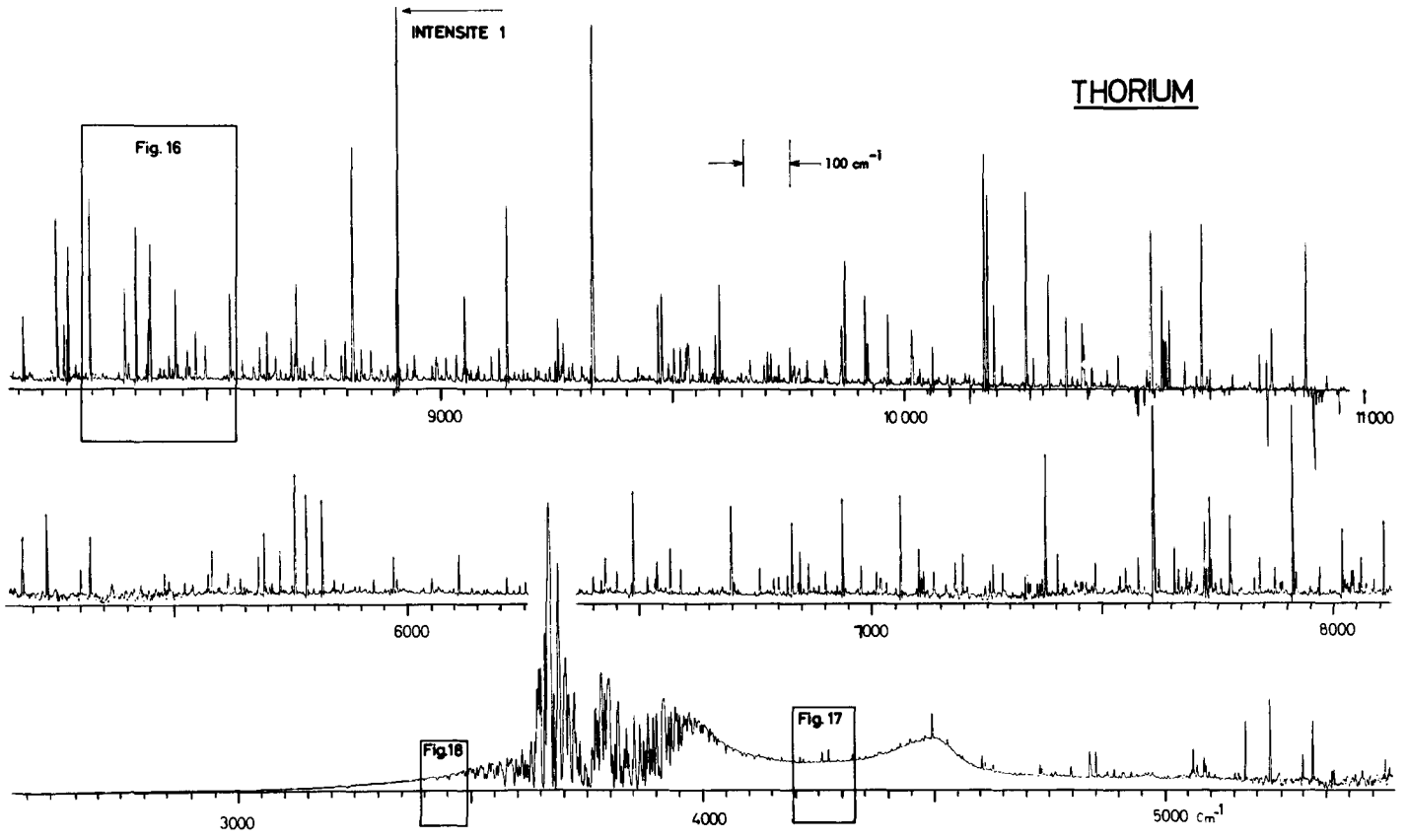

Fig. 15. Spectrum of thorium computed from the first 10^4 points of an interferogram of 10^6 points. The resolution indicated is $\delta\sigma = 2\ cm^{-1}$. For all these spectra, including those following, the reference wavelength is not known precisely and the data have not been corrected for the refractive index of the atmosphere. Consequently, the wave number scale is provisional only.

NOTE: INTENSITE 1 = unit intensity, the peak to which this and all subsequent traces are normalized.

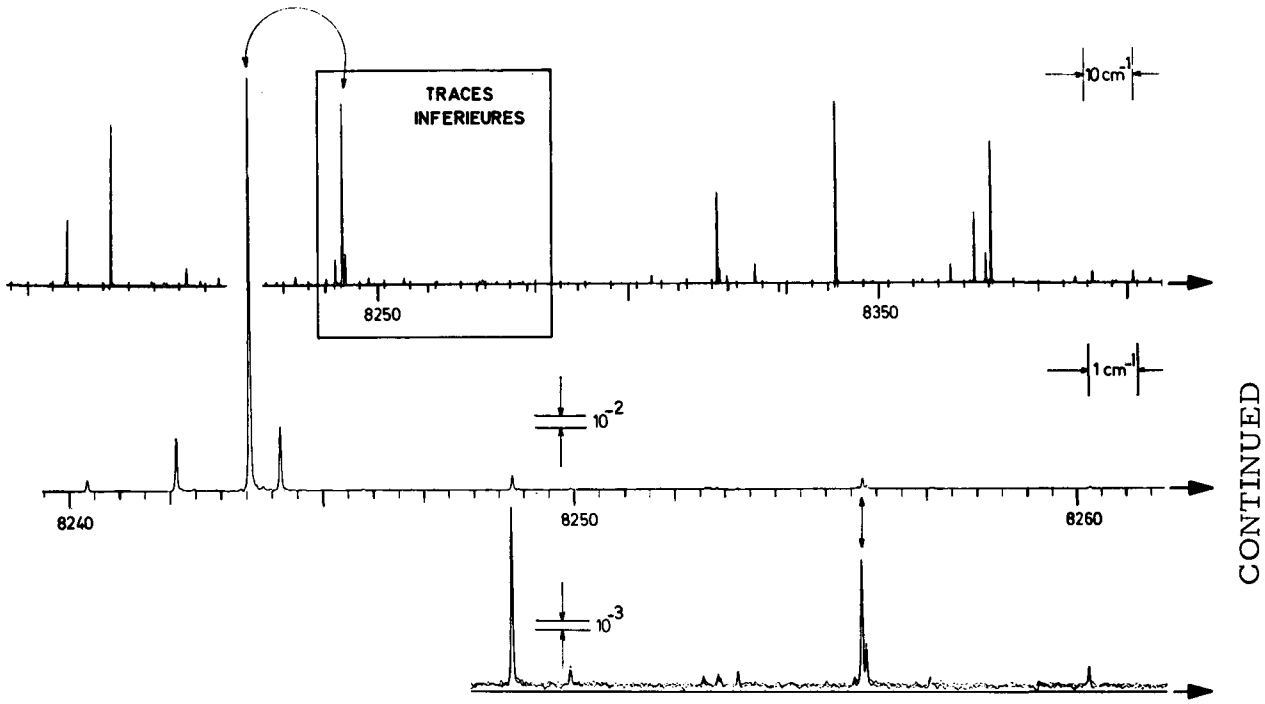

Fig. 16. Spectrum of thorium (same interferogram as for Fig. 15)

On Top: the spectral region indicated in Fig. 15, calculated from 10^5 points ($\delta\sigma$ = 0.2 cm^{-1}).

Middle: 40 cm^{-1} slice calculated from 10^6 points ($\delta\sigma$ = 0.02 cm^{-1})

Bottom: Same region and abscissas, but the vertical scale multiplied by 10. A second spectrum recorded under the same conditions is superposed on the first. On this scale, the entire spectrum would be 80 meters long.

NOTE: TRACES INFERIEURES = lower traces

FROM PRIOR PAGE

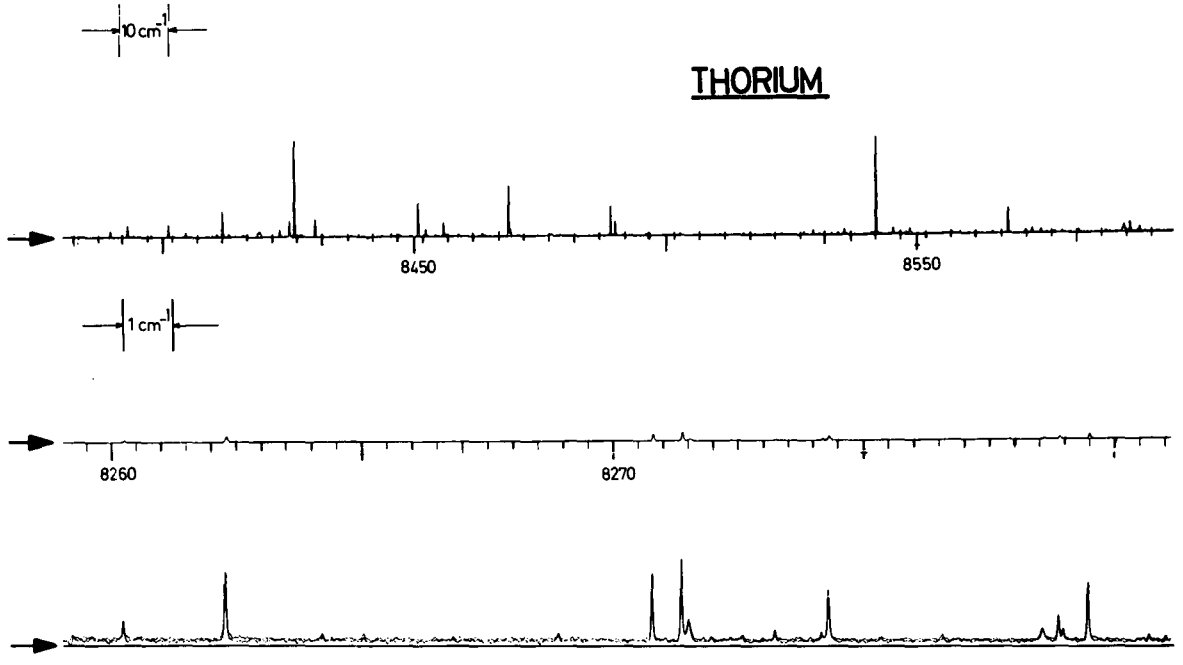

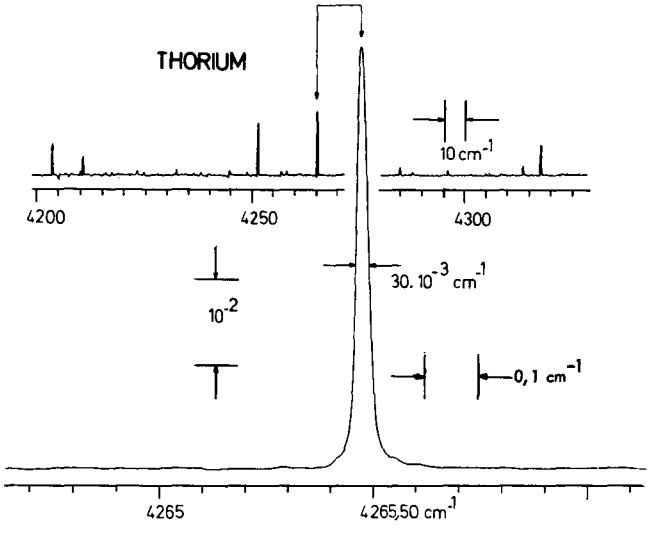

Fig. 17. Spectrum of thorium

Above: a region indicated on Fig. 15, calculated from 10^5 points ($\delta\sigma$ = 0.2 cm^{-1})

Below: a single line calculated from 10^6 points ($\delta\sigma$ = 0.02 cm^{-1}) showing essentially a Lorentz profile.

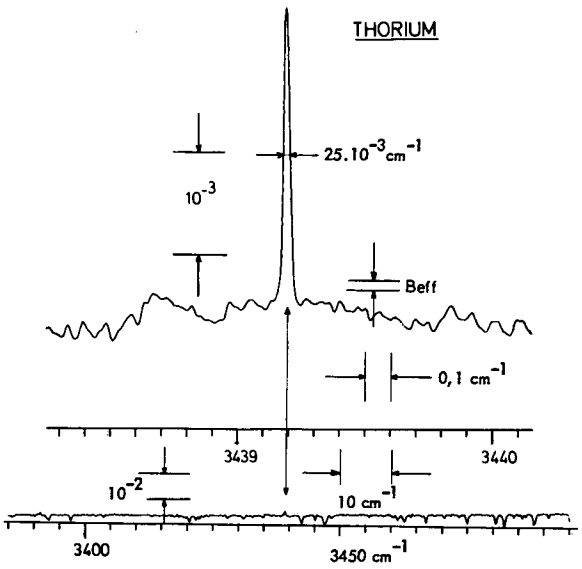

Fig. 18. Spectrum of thorium

Below: the region indicated in Fig. 15, calculated from 10^5 points ($\delta\sigma = 0.2\ cm^{-1}$)

Above: a very weak line calculated from 10^6 points and showing the smallest width observed ($0.025\ cm^{-1}$).

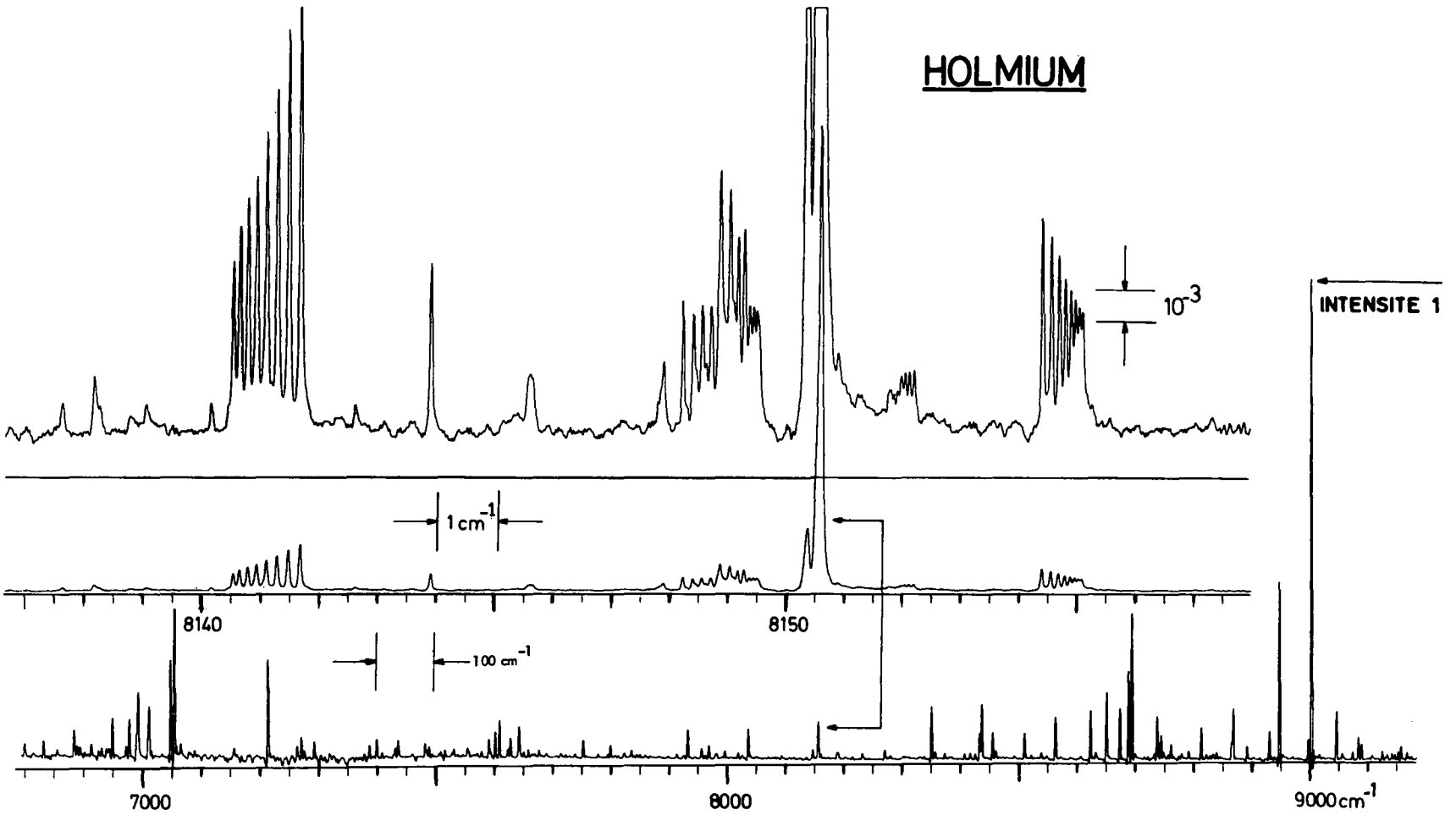

Fig. 19. Spectrum of holmium

Bottom: trace computed from 10^4 points (as Fig. 15) ($\delta\sigma$ = 2 cm^{-1})

Middle: 20 cm^{-1} slice computed from 10^6 points ($\delta\sigma$ = 0.02 cm^{-1})

Above: Same region, same resolution, ordinate expanded by a factor of 10.

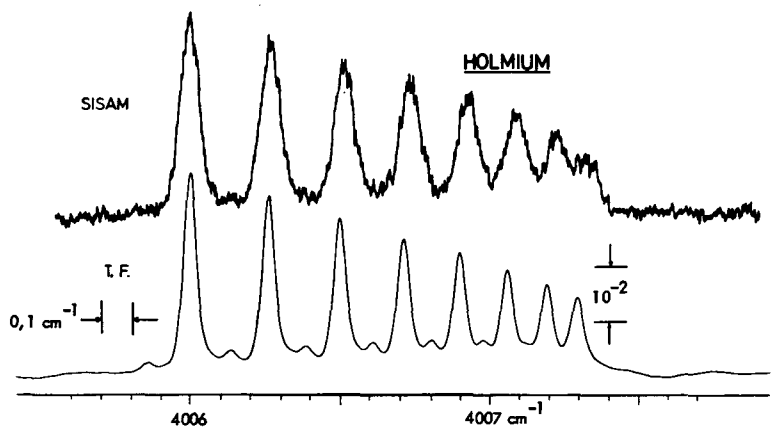

Fig. 20. Spectrum of holmium

Above: the weakest hyperfine structure of holmium recorded with a SISAM ($\delta\sigma$ = 0.03 cm^{-1}, recording time 30 minutes)

Below: same structure recorded by Fourier spectroscopy (same interferogram as for Fig. 19; $\delta\sigma$ = 0.02 cm^{-1}). The entire spectrum is 320 m long.

VI. CONCLUSION

These first results have established the possibility of attacking problems needing high resolution and very wide spectral range using Fourier spectroscopy. In the case of complex emission spectra, the information contained in one 10^6-point interferogram surpasses both in quantity and quality that produced by existing methods in the course of research programs lasting several months. The calculated spectrum is available on a magnetic tape in a format directly usable by the computer, and programs exist that automatically detect and measure the position and intensity of lines (Ref. 8).

The next stage should be to undertake the measurement of absolute frequencies, which will require that the interferometer control system operate from an international standard Krypton lamp. The interferometer will, eventually, be tried in the visible; its performance must then be compared to that of a large crossed-grating spectrograph with a Fabry-Perot etalon, compared to which there is no question of being able to obtain a significant speed gain. An increase in the number of samples to $N = 5 \times 10^6$ seems conceivable without modification of the instrument; spectroscopic problems justifying such an expansion are doubtless rare.

A real-time digital computer, specially adapted to the interferometer, is also in the process of construction.* It uses the classical algorithm (that of Cooley and Tukey not being usable in a real-time calculation). The basic cycle-time is 1 μm s/input point/output point; thus it is, for this particular problem, 1000 times faster than the 7040 (Table 1, column 2, and Fig. 14, the curve labeled "7040 classique") and about 100 times faster than the 360/75. It can calculate up to 20,000 points in a spectrum starting from an interferogram recorded at a rate of 50 points/second, without any limitation on N. In itself sufficient for all problems in which $M < 20,000$, in other cases it allows a portion of the spectrum to be examined in real time.

*Translator's Note: This device was successfully completed early in 1971.

We wish to thank M. Ubelmann for his salutory help in setting up and testing the interferometer, M. Calvignac for the mechanical design, MM. Seguin, Durand and Dessens, who were largely responsible for the difficult and delicate task of producing the electronic system, M. Collet for the magnetic tape reading and conversion program, and all the personnel of CIRCE.

REFERENCES

1. Connes (J.), Connes (P.). -- J.O.S.A., 1966, 56, 896.

2. Connes (J.), Connes (P.), Maillard (J.P.). -- J. Phys., 1967, 28, C2, 120.

3. Maillard (J.P.). -- Thèse, Fac. des Sciences d'Orsay, 1967.

4. Cuisenier (M.), Pinard (J.). -- J. Phys., 1967, 28, C2, 97.

5. Mertz (L.). -- J. Phys., 1967, 28, C2, 87 et Mertz (L.). -- Astr. J., 1966, 70, 548.

6. Forman (M.L.). -- J. Phys., 1967, 28, C2, 58.

7. Connes (J.), Connes (P.). -- J. Phys., 1967, 28, C2, 57.

8. Delouis (H.). -- Thèse, Faculté des Sciences d'Orsay, 1968.

9. Connes (J.), Connes (P.), Maillard (J.P.). -- Atlas des spectres dans le proche infrarouge de Vénus, Mars, Jupiter et Saturne. Editions du C. N. R. S., 1969.

10. Pinard (J.). -- J. Phys., 1967, 28, C2, 136.

11. Pinard (J.). -- Thèse, Ann. Phys., 1969, n° 2 (à paraître).

12. Connes (J.). -- Rev. Opt., 1961, 40, 45, 116, 171, et 231.

13. Bridges (T. J.), Kluvier (J.W.). -- App. Opt., 1965, 4, 1121.

14. De Lang (H.), Bouwhuis (G.). -- Philips Tech. Rev., 1969, 30, 160.

15. Connes (P.). -- Rev. Opt., 1959, 38, 157 et 416; 1960, 39, 402.

16. Giacchetti (A.), Stanley (R.W.), Zalubas (R.). -- J.O.S.A., (sous presse).

17. Steers (F.B.M.). -- Spectrochim. Act., 1967, 23B, 135.

18. Rao (K.N.), Humphreys (C.S.), Rank (D.H.). -- Wavelength standards in the infrared, Academic Press, 1966.

19. Verges (J.). -- Thèse, Fac. des Sciences d'Orsay, 1969.

20. Verges (J.). -- Spectrochim. Act., 1969, 24B, 177.

21. Camus (P.), Guelachvili (G.), Verges (J.). -- Spectrochim. Act., 1969, 24B, 373.

22. Blaise (J.), Morillon (C.), Schweigofer (M.G.), Verges (J.). -- Spectrochim. Act., 1969, 24B, 405.

23. Morillon (C.). -- Spectrochim. Act., (sous presse).

24. Cooley (J.W.) et Tukey (J.W.). -- Mathematics of computation (1965), 19, 296.

25. Cooley (J.W.) et Brenner (N.M.). -- Communication privée.

26. Cochran (W.T.), Cooley (J.W.). -- IEE Trans. Aud. El. Acous., 1967, AU-15, 2, 45.

NASA — JPL — Coml., L.A., Calif.